

analysis was used to show that the effects are not due to sulfur or carbon diffusing to the surface. Also, the process is reversible; room-temperature data is repeated when the sample cools to room temperature.

Presumably, the surface-state binding energy decreases with increasing temperature permitting electrons to spill out of this state and thus reducing its emission amplitude. The fact that an observable shoulder remains at 400 °C (above the Curie temperature) indicates that the temperature-dependent shift in binding energy for this surface state is less than its binding energy, but clearly not zero.

In summary, this paper reports a previously unobserved feature in the Ni(100) photoemission spectra. Within experimental limits this feature satisfies all conditions for a surface state, and it is identified as resulting from a *magnetic* surface state near $\bar{\Gamma}$. This new result places important constraints on the interpretation of ESP experiments in terms of bulk band structure.

It is a pleasure to acknowledge many helpful discussions with L. Kleinman, and support from the Research Corporation, and the National Science Foundation under Grant No. DMR-79-23629.

¹W. Eib and F. S. Alvarado, Phys. Rev. Lett. **37**,

444 (1976).

²N. V. Smith and S. Chiang, Phys. Rev. B **10**, 5013 (1979).

³I. D. Moore and J. B. Pendry, J. Phys. C **11**, 4615 (1978).

⁴F. J. Himpsel, J. A. Knapp, and D. E. Eastman, Phys. Rev. B **19**, 2919 (1979).

⁵D. G. Dempsey and L. Kleinman, Phys. Rev. Lett. **39**, 1297 (1977); D. G. Dempsey, W. R. Grise, and L. Kleinman, Phys. Rev. B **18**, 1270 (1978).

⁶C. S. Wang and J. Callaway, Phys. Rev. B **15**, 298 (1977).

⁷A. Liebsch, Phys. Rev. Lett. **43**, 1431 (1979).

⁸L. Kleinman, Phys. Rev. B **19**, 1295 (1979).

⁹E. W. Plummer and W. Eberhardt, Phys. Rev. B **20**, 1444 (1979).

¹⁰N. Shevchik, J. Electron Spectrosc. **14**, 411 (1978).

¹¹The resonance lamp radiation was not polarized.

At $\hbar\omega = 21.2$ eV, incident angles corresponding to $k_{\parallel} = 0.0 \text{ \AA}^{-1}$, 0.35 \AA^{-1} , and 0.69 \AA^{-1} were 33° , 23° , and 3° which produce incident "p" components of approximately 27%, 20%, and 2% of the total field.

¹²Resolution in the retardation mode is given by $0.007E_p$ (small aperture) or $0.02E_p$ (large aperture), where E_p = pass energy of the analyzer. Based on source size and pass-energy settings, selected spectra were obtained using an estimated resolution of approximately 40 meV. These spectra did not differ from spectra taken with use of an estimated resolution of approximately 60 meV. At values of resolution worse than 100 meV the Fermi edge smears out and the resolved peak at E_F becomes a shoulder (at what appears to be a higher binding energy; see Ref. 9).

Observation of the Meissner Effect in an Organic Superconductor

K. Andres, F. Wudl, D. B. McWhan, G. A. Thomas, D. Nalewajek, and A. L. Stevens

Bell Laboratories, Murray Hill, New Jersey 07974

(Received 5 September 1980)

A partial Meissner effect, fully diamagnetic shielding signals, and large anisotropies in the upper and lower critical fields in ditetramethyltetraselenafulvalene-hexafluorophosphate [(TMTSF)₂PF₆] under applied hydrostatic pressure are observed.

PACS numbers: 74.30.Ci, 72.80.Le, 74.70.Rv

The compound ditetramethyltetraselenafulvalene-hexafluorophosphate [(TMTSF)₂PF₆] is a highly conducting linear-chain organic crystal. At atmospheric pressure, Bechgaard *et al.*¹ have observed a conductivity $\sigma \approx 10^5 (\Omega \text{ cm})^{-1}$ near a temperature of 20 K. Below about 15 K the material enters a semiconducting state which resembles the Peierls state observed in a number of similar compounds.² At a hydrostatic pressure $P = 1.2$ GPa, Jerome *et al.*³ have found that the semiconducting transition is absent and that there

is a new transition at 0.9 K where σ increases by over 10^5 . With the application of magnetic fields of order 200 Oe, the transition temperature T_c drops, and the magnitude of the rise in σ decreases to ~ 5 . Subsequent ac susceptibility measurements⁴ at a frequency $\nu = 68$ Hz show an anomaly indicative of a transition into a diamagnetic state. Jerome *et al.*³ have suggested that (TMTSF)₂PF₆ at $P = 1.2$ GPa is a BCS superconductor.⁵

Although there have been several theoretical models for high conductivity in one-dimensional

organic compounds, such as sliding charge-density waves⁶⁻⁹ or excitonic exchange,¹⁰ (TMTSF)₂-PF₆ appears to be the first experimental realization of superconductivity in an organic compound. It should be noted, however, that all of the observations mentioned above could result from filamentary or surface superconductivity. In contrast, the Meissner effect^{5,11} (i.e., flux expulsion on cooling in a field) is a unique feature of bulk superconductivity. We have observed this effect in crystals of (TMTSF)₂PF₆ under conditions similar to those of Jerome *et al.*³

Samples of (TMTSF)₂PF₆ were grown electrochemically, either from distilled chlorobenzene or methylene chloride (stored over alumina) with use of twice-recrystallized tetrabutylammonium hexafluorophosphate as electrolyte. The donor TMTSF was sublimed at 10⁻² Torr until further sublimations left no residue in the pot. Crystal growth occurred over about 10-14 d at 1-3 μA and 0.6 V.

A beryllium-copper clamp device¹² was used to generate pressures up to 2 GPa, and was cooled to $T \geq 20$ mK in a dilution refrigerator. Two superconducting coils were contained inside a Teflon cell 0.635 cm in diameter and 2.3 cm long, which was filled with a 50-50 pentane-2-methylbutane mixture. Up to seven wires were brought into the cell, through a standard epoxy seal. A novel superconducting bridge circuit with a SQUID detector was used for measuring the changes in sample magnetization. The bridge circuit, shown in the upper right inset of Fig. 1, consists of two (upper) transformer coils and three (lower) sample coils, the latter of which are made of 100 turns of niobium wire each and are 0.4 cm long with an inside diameter of 0.1 cm. Supercurrents i_{s1} and i_{s2} , induced by the corresponding primary currents in the upper coils, generate the measuring fields in the sample coils. Any flux change in a sample in one of these coils causes a corresponding change in supercurrent flowing through that coil and through the SQUID sensor. The dashed line in the figure indicates the two sample coils inside the pressure cell. The third sample coil was used for a Sn reference whose superconducting transition temperature relative to a Sn sample inside the cell was used to calibrate the pressure. A Permendur shield around the cryostat reduced Earth's field to a few millioersteds. The remaining field component in the coil axis can be further compensated by finding that supercurrent which minimized the Meissner signal of the Sn transition. For magnetization measure-

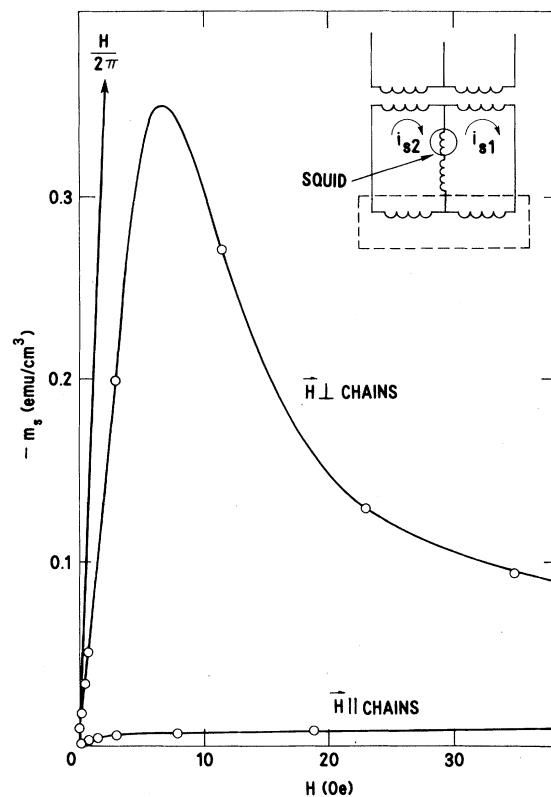


FIG. 1. Diamagnetic magnetization vs applied field at $T = 0.2$ K for fields oriented parallel and perpendicular to the linear chain axis of the crystals. The straight line is the initial slope for H_{\parallel} . The inset on the upper right shows the SQUID bridge circuit (see text).

ments in transverse fields, oval-shaped (flattened) niobium coils were used into which the needlelike crystals were placed with the chain axis perpendicular to the coil axis. Fields up to ~ 150 Oe could be generated in these small coils. Larger fields were provided by a superconducting solenoid located in the helium bath and oriented coaxially with the small niobium coils.

Two of our observations of persistent shielding currents and of the Meissner effect are shown in Fig. 2, for transverse measuring field H_{\perp} . The sample was first cooled below T_c in zero field, then H_{\perp} was applied (see arrow) and the shielding currents measured. The sample was then warmed to monitor the change in these currents (upper curve, Fig. 2). In the same field, finally the sample was cooled again to observe the Meissner effect. The diamagnetic susceptibility plotted in Fig. 2 is normalized to $-1/2\pi$ appropriate for the demagnetization factor¹¹ of a cylinder in H_{\perp} (rather than $-1/4\pi$ for H_{\parallel}). We observe full diamag-

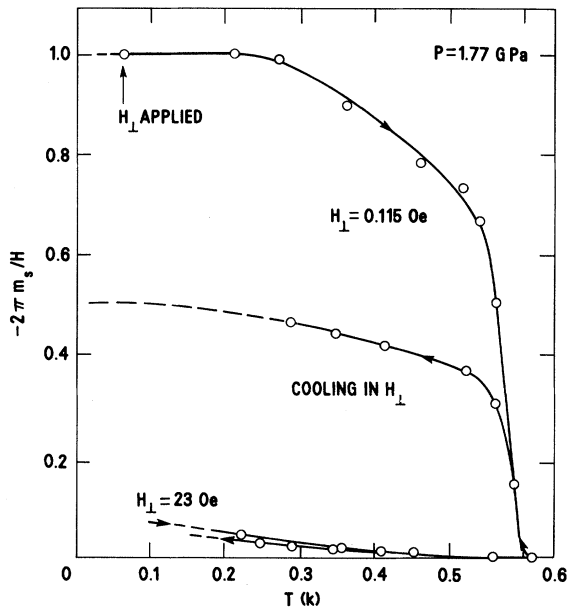


FIG. 2. Observed diamagnetic susceptibilities after cooling in $H=0$ and then applying a field transverse to the chain axis (warming curves) and for cooling below the superconducting transition in an applied field. Curves are shown for two values of H_{\perp} .

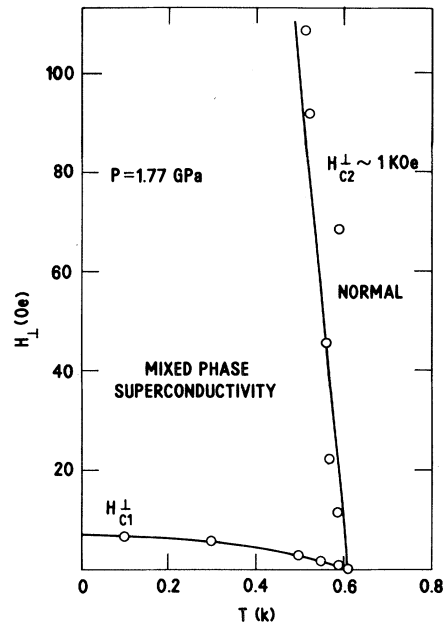


FIG. 3. $H_c - T_c$ phase diagram for perpendicular field.

netic shielding signals (with an uncertainty of 15%, as determined by comparison with the Sn reference) and a Meissner effect of about 50% for $H_{\perp} \leq 3$ Oe. For $H_{\perp} > 3$ Oe, both the shielding signal and the Meissner signal decrease rapidly in amplitude, while the transition temperature remains roughly unchanged, as illustrated by the 23-Oe data in Fig. 2. A similar reduction of the shielding currents is observed for H_{\parallel} .

In Fig. 1, the Meissner magnetization m_s at $T = 0.2$ K is plotted versus applied field for both H_{\perp} and H_{\parallel} . For H_{\perp} , m_s is similar to that of conventional type-II superconductor. We take the field at which the first departure from linearity of m_s vs H occurs as an estimate of H_{c1} . For H_{\perp} , this field (times 2 for the demagnetization factor) gives $H_{c1} \sim 5$ Oe at 0.2 K and is illustrated for various values of T in Fig. 3. Since our SQUID system only works up to ~ 200 Oe, we have used the initial depression of T_c with H_{\perp} (Fig. 3; similar to that observed by Jerome *et al.*³) to estimate a transverse $H_{c2} \sim 500-1000$ Oe.

The measurements in H_{\parallel} (made on samples from a different batch of samples prepared in the same way) show an entirely different behavior¹³ from that in H_{\perp} . In this case, a maximum Meissner effect of only 8% is found. The value of

H_{c1} for H_{\parallel} is only ~ 0.5 Oe and the magnetization rises monotonically to a nearly field-independent value which is larger than in the transverse case. We have also monitored the resistivity in H_{\parallel} of a thin ($0.0018 \times 0.0076 \times 0.25$ cm³) crystal from the same batch, from which we find the parallel $H_{c2} = 7.2 \pm 0.2$ kOe. The critical fields thus suggest

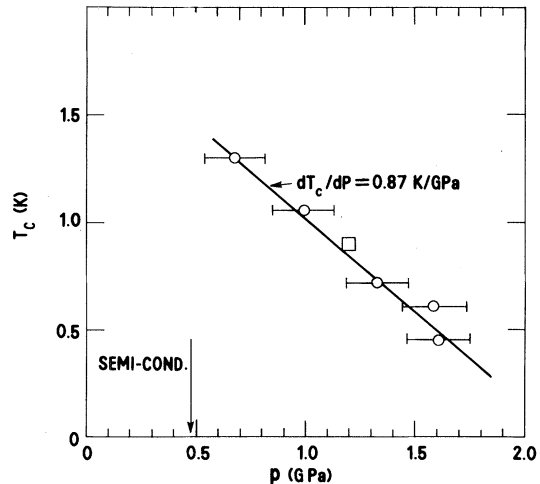


FIG. 4. Observed pressure dependence of the superconducting transition temperature of $(TMTSF)_2PF_6$. The result observed by Jerome *et al.* (Ref. 3) is indicated by the open square. The arrow at $P = 0.48$ GPa indicates that the sample becomes semiconducting at $T = 4.2$ K and shows no superconductivity above 20 mK.

an anisotropy of about a factor of 6.5 in the κ parameter of type-II superconductivity.¹¹ One peculiar property of superconducting (TMTSF)₂PF₆ is that three-dimensional shielding currents are reduced in magnitude in very low applied fields, which means that the critical supercurrent density must be very low in at least two directions, probably transverse to the chain axis. From all our T_c vs P data we find a strong dependence of T_c on pressure, as is shown in Fig. 4.

In conclusion, we have shown that (TMTSF)₂PF₆ under pressure is a bulk superconductor in near-zero field which exhibits rather unusual and very anisotropic properties in applied fields. We wish to thank P. W. Anderson, E. I. Blount, and C. M. Varma for helpful comments.

¹K. Bechgaard, C. S. Jacobsen, K. Mortensen, H. J. Pedersen, and N. Thorup, *Solid State Commun.* **33**, 1119 (1980).

²*The Physics and Chemistry of Low Dimensional Solids*, edited by L. Alcacer (Reidel, Hingham, Mass.,

1980).

³D. Jerome, A. Mazaud, M. Ribault, and K. Bechgaard, *J. Phys. Lett.* **41**, L95 (1980).

⁴M. Ribault, G. Benedek, D. Jerome, and K. Bechgaard, *J. Phys. Lett.* **41**, L397 (1980).

⁵J. Bardeen, L. N. Cooper, and J. R. Schrieffer, *Phys. Rev.* **108**, 1175 (1957).

⁶H. Fröhlich, *Proc. Roy. Soc. London, Sect. A* **223**, 296 (1954).

⁷P. W. Anderson, P. A. Lee, and M. Saitoh, *Solid State Commun.* **13**, 595 (1973).

⁸D. Allender, J. W. Bray, and J. Bardeen, *Phys. Rev. B* **9**, 119 (1974).

⁹P. A. Lee and T. M. Rice, *Phys. Rev. B* **19**, 3970 (1979), and references therein.

¹⁰W. A. Little, *Phys. Rev.* **134**, A1416 (1964).

¹¹See, for example, *Superconductivity*, edited by R. D. Parks (Dekker, New York, 1969).

¹²C. W. Chu, L. R. Testardi, F. J. Di Salvo, and D. E. Moncton, *Phys. Rev. B* **14**, 464 (1976).

¹³In both the shielding and Meissner signals of this sample and the resistivity of a similar sample, we see evidence of two transition temperatures, a sharp one at 0.7 K and a broader one below 0.6 K. K. Andres, F. Wudl, D. B. McWhan, G. A. Thomas, D. Nalewajek, and A. L. Stevens, to be published.

Island Growth and Orientational Locking of Potassium Intercalated in Graphite

A. N. Berker,^(a) N. Kambe,^(b) G. Dresselhaus,^(c) and M. S. Dresselhaus^(b)
*Center for Materials Science and Engineering, Massachusetts Institute of Technology,
 Cambridge, Massachusetts 02139*
 (Received 29 April 1980)

Island growth and orientational locking in stage-2 potassium-intercalated graphite is observed by real-space imaging and electron diffraction on single crystallites. A mechanism is presented, relating these two phenomena. For $86 \lesssim T \lesssim 130$ K, intercalate islands of incommensurate ordering are orientationally unlocked from the graphite lattice, as indicated by ring diffraction patterns. With increasing temperature, gradual island growth is by accretion. A threshold size (~ 50 Å reached at 130 K) triggers precipitous island growth by coalescence and orientational locking.

PACS numbers: 81.30.Hd, 61.16.Di, 64.70.Kb, 68.55.+b

Intercalate systems, in addition to their inherent materials science interest, provide a new arena for the study of phase transitions and critical phenomena, involving a large variety of possible phases¹ and, presumably, new phenomena where these phases meet. Whereas recent studies²⁻⁴ of these systems have almost uniformly interpreted experimental data in terms of single homogeneous phases, this Letter describes, for stage $n=2$ potassium in graphite, the necessary and interesting coexistence of distinct regions which differ in intercalate concentration and structure. We report electron diffraction meas-

urements which probe a single graphite crystallite within highly oriented pyrolytic graphite, in the temperature range of $5 < T < 800$ K. These measurements are supplemented by bright-field and dark-field real-space images of the crystallite. The experiments show, for intermediate⁵ temperatures $86 < T < 130$ K, the occurrence of small "islands" of positional order incommensurate⁶ to graphite basal structure, in a "sea" of disorder. These islands are orientationally unlocked from the graphite and, therefore, from each other, as indicated by a diffraction pattern of six to eight discernible sharp rings [Fig. 1(b)], which are